Residues in the ϵ Subunit of the Nicotinic Acetylcholine Receptor Interact To Confer Selectivity of Waglerin-1 for the α−ϵ Subunit Interface Site†

Brian E. Molles,‡,§ Igor Tsigelny,‡ Phuong D. Nguyen,‡ Sarah X. Gao,‡ Steven M. Sine,|| and Palmer Taylor*,‡

Department of Pharmacology and Biomedical Sciences Graduate Program, University of California at San Diego, La Jolla, California 92093-0636, and Receptor Biology Laboratory, Department of Physiology and Biophysics, Mayo Foundation, Rochester, Minnesota 55905

Received February 25, 2002; Revised Manuscript Received April 29, 2002

ABSTRACT: Waglerin-1 (Wtx-1) is a 22-amino acid peptide that competitively antagonizes muscle nicotinic acetylcholine receptors (nAChRs). Previous work demonstrated that Wtx-1 binds to mouse nAChRs with higher affinity than receptors from rats or humans, and distinguished residues in α and ϵ subunits that govern the species selectivity. These studies also showed that Wtx-1 binds selectively to the α−ϵ binding site with significantly higher affinity than to the α−δ binding site. Here we identify residues at equivalent positions in the ϵ, γ, and δ subunits that govern Wtx-1 selectivity for one of the two binding sites on the nAChR pentamer. Using a series of chimeric and point mutant subunits, we show that residues Gly-57, Asp-59, Tyr-111, Tyr-115, and Asp-173 of the ϵ subunit account predominantly for the 3700-fold higher affinity of the α−ϵ site relative to that of the α−γ site. Similarly, we find that residues Lys-34, Gly-57, Asp-59, and Asp-173 account predominantly for the high affinity of the α−ϵ site relative to that of the α−δ site. Analysis of combinations of point mutations reveals that Asp-173 in the ϵ subunit is required together with the remaining determinants in the ϵ subunit to achieve Wtx-1 selectivity. In particular, Lys-34 interacts with Asp-173 to confer high affinity, resulting in a $\Delta\Delta G_{INT}$ of −2.3 kcal/mol in the ϵ subunit and a $\Delta\Delta G_{INT}$ of −1.3 kcal/mol in the δ subunit. Asp-173 is part of a nonhomologous insertion not found in the acetylcholine binding protein structure. The key role of this insertion in Wtx-1 selectivity indicates that it is proximal to the ligand binding site. We use the binding and interaction energies for Wtx-1 to generate structural models of the α−ϵ, α−γ, and α−δ binding sites containing the nonhomologous insertion.

The nicotinic receptor contains five separate polypeptide subunits arranged with radial symmetry around a central channel (*1*, *2*). The five subunits in the muscle receptor, two copies of α and one each of β, δ, and γ (embryonic subtype) or ϵ (adult subtype) (*3*), assemble in the following counterclockwise order: α−γ/ϵ−α−δ−β. The crystal structure of the acetylcholine binding protein (AChBP)[1] from the freshwater snail *Lymnaea stagnalis* (*4*, *5*) firmly establishes binding site location and subunit handedness in the nAChR by demonstrating that binding site residues contributed by the α subunit contribution are found on the "clockwise" face of the AChBP subunit, and the non-α subunit residues contributing to the binding site are found on the "counterclockwise" face of the AChBP subunit (*6*).

The two binding sites for agonists, reversible competitive antagonists and the pseudo-irreversible α-bungarotoxin (α-BgTx), are formed at α−δ and α−ϵ (or α−γ) subunit interfaces of the muscle receptor. Mutagenesis and site-directed labeling studies established that seven segments, far apart in the linear sequence, contribute to the ACh binding site: segments A−C in the α subunit and segments D−G in δ, ϵ, or γ subunits (*1*, *2*). The AChBP structure confirmed that residues in each of these segments are present at the ACh binding site, establishing it as a template for the tertiary structure of the major extracellular domain.

Each of the five subunits of the muscle nAChR contains between 445 and 497 amino acids. Each subunit has one to three N-linked glycosylation sites and four transmembrane spans, giving the pentamer a molecular mass of nearly 300 kDa. Its large size and amphipathic character make the nAChR refractory to crystallization and NMR spectroscopy aimed at determining its atomic structure.

Isolated from the venom of Wagler's pit viper, *Tropidolaemus wagleri* (*7*), the waglerin peptides are remarkably selective peptide antagonists. Site-selective antagonists are significant because although binding of two agonist molecules is required to activate the receptor, binding of a single agonist molecule blocks activation. The four closely related waglerins are the only characterized toxins from the Viperidae family of snakes that target nicotinic receptors; waglerin-1 (Wtx-1) has the sequence NH_2-GGKPDLRPCH-

† This work was supported by Grants GM18360 to P.T., GM07752 to B.E.M., and NS31744 to S.M.S.

* To whom correspondence should be addressed.

‡ Department of Pharmacology, University of California at San Diego.

§ Biomedical Sciences Graduate Program, University of California at San Diego.

|| Mayo Foundation.

[1] Abbreviations: nAChR, nicotinic acetylcholine receptor; [^{125}I]-α-BgTx, [^{125}I]-α-bungarotoxin; AChBP, acetylcholine binding protein; Wtx-1, waglerin-1.

10.1021/bi025732d CCC: $22.00
Published on Web 05/29/2002

PPCHYIPRPKPR-COOH. A single intramolecular disulfide bond forms between the two Cys residues, as determined by NMR spectroscopy (*8*, *9*). Wtx-1 binds to the adult mouse AChR with 2100-fold higher affinity for the α−ϵ over the α−δ binding site (*10*). In this regard, Wtx-1 joins D-tubocurarine (*11*), α-conotoxin MI (*12*, *13*), and *Naja mossambica mossambica* α-neurotoxin (*14*) as highly site-selective prototype competitive antagonists against mammalian muscle receptors. Studies using these ligands demonstrated that the ligand binding sites are formed at interfaces between α and non-α subunits (*11*, *13*−*16*). By quantification of contributions of individual residues to site selectivity for these ligands, residues on both the α and non-α subunits have been shown not only to be proximal to the bound ligand but also to govern the shape of the binding site and orientation of bound ligand.

Here we use chimeric and point mutant subunits to identify residues in mouse ϵ, γ, and δ subunits that confer binding site selectivity for Wtx-1. Analysis of combinations of point mutations demonstrates that several of these determinants of ligand selectivity are energetically coupled, revealing cooperative participation in ligand recognition. Energetic coupling suggests the proximity of these residues to each other and to the ligand binding site, which enabled modeling of the binding sites using the crystal structure of AChBP (*4*, *5*) as a template.

EXPERIMENTAL PROCEDURES

Synthesis and Purification of Waglerin-1. The crude peptides, synthesized by American Peptide Co. (San Jose, CA) or Synpep (Dublin, CA), were dissolved to a concentration of 0.8 mg/mL in 30 mM Tris-HCl (pH 8.2−8.5), sterile filtered, and left overnight at room temperature for formation of the single intramolecular disulfide bond in the Wtx-1 structure. After disulfide bond cyclization, 0.1% trifluoroacetic acid was added to minimize the formation of intermolecular disulfide bonds. Peptide solutions (2 mL) were loaded onto a 5 mL HPLC sample loop leading to a 10 mm × 250 mm semipreparative reverse-phase C18 column (Vydac), with 0.1% trifluoroacetic acid as solvent A and 0.085% trifluoroacetic acid and 70% acetonitrile as solvent B. Elution was achieved by increasing the level of solvent B from 20 to 25% over the course of 15 min. The cyclized peptide elutes 1−2 min earlier than uncyclized peptides or dimerized peptides formed by intermolecular disulfide bond formation (*17*). Fractions containing the purified peptide were pooled and lyophilized. Representative samples from different lots were checked for purity and correct mass by MALDI or ion-spray mass spectrometry.

Mutagenesis of nAChR Subunits. Cloned cDNAs for mouse α (*18*), β (*19*), γ (*20*), δ (*21*), and ϵ subunits (*22*) were ligated into the mammalian expression vector pRBG4 at *Eco*RI sites for transient expression in HEK293 cells (*11*). Site-specific mutants of the wild-type mouse γ, δ, or ϵ subunit were made by one of two methods. Complementary synthetic oligonucleotides (Sigma/Genosys, The Woodlands, TX) containing the desired mutation were ligated into the cDNA at unique restriction sites flanking the mutated region. When convenient restriction sites were not available, the Stratagene double primer method was used. In this procedure, complementary oligonucleotides containing the desired mutation served as primers in a PCR amplification reaction that included the wild-type plasmid and *Pfu* polymerase. Following 16−18 amplification cycles to make the entire plasmid, the reaction mixture was treated with *Dpn*I restriction endonuclease to digest only the methylated, wild-type plasmid DNA, leaving behind the newly synthesized DNA. Mutations were subcloned into vectors not subjected to mutagenesis and verified initially by restriction digests and then by DNA sequencing. Large-scale plasmid preparations used DEAE columns (Gibco or Qiagen) or cesium chloride ultracentrifugation for purification.

Transfections. The individual subunit cDNAs for the nAChR are contained on unique plasmids using the CMV promoter-based pRBG4 vector (*23*). HEK293 cells were transfected by the calcium phosphate method; the medium was changed 12−16 h later, and binding assays were performed 1−2 days after the medium change. Expression levels that allowed an estimation of Wtx-1 K_D values ranged from 60 to 950 fmol per 10 cm plate of cells.

Estimation of Waglerin-1 K_D Values by Competition with the Initial Rate of [^{125}I]-α-Bungarotoxin ([^{125}I]-α-BgTx) Binding. Transfected cells were removed from the culture plates by gentle agitation with 5 mL of phosphate-buffered saline (pH 7.4) containing 5 mM EDTA. After incubation of the dissociated cells with waglerin-1 for 45 min to 1 h, 5 nM [^{125}I]-α-BgTx (New England Nuclear) was added and allowed to incubate for 30 min such that 30−50% of the available binding sites become occupied (*24*). Waglerin dissociation constants were determined from the fractional reduction of the initial rate of [^{125}I]-α-BgTx binding. The total number of sites was determined by incubating with 20 nM [^{125}I]-α-BgTx for 1 h. The level of nonspecific binding was determined by incubating the cells with 10 mM carbachol before reacting with [^{125}I]-α-BgTx. Transformed data were fit to either the one-site or two-site Hill equation using Prism 2.0 (Graphpad).

Receptor Model Construction. The receptor was modeled structurally against the crystallographic coordinates of the acetylcholine binding protein (PDB entry 1i9b) using the program Homology and Insight II (Accelrys, 2000). The receptor structure was then energy minimized for 10 000 iterations of conjugated gradients using a distance-dependent dielectric constant with the program Discover (Accelrys, 2000).

RESULTS

Throughout this investigation, our working hypothesis is the protein scaffolds of the ϵ, γ, and δ subunits are, to a first approximation, superimposable; residues at homologous positions in the primary sequences occupy equivalent locations in three-dimensional coordinate space. Because each of these non-α subunits partners with an α subunit to form a binding site, they are the predominant sources of binding site selectivity for Wtx-1. Therefore, to identify determinants of Wtx-1 selectivity, our experiments seek to reconstitute binding affinity conferred by one non-α subunit by residue substitution into the template of another. In particular, we convert selectivity of the ϵ subunit into γ- and δ-like subunit, and convert the γ and δ subunit selectivity into an ϵ-like subunit.

γ−ϵ Subunit Determinants for Waglerin. Because the γ and ϵ subunits show the highest level of identity among the

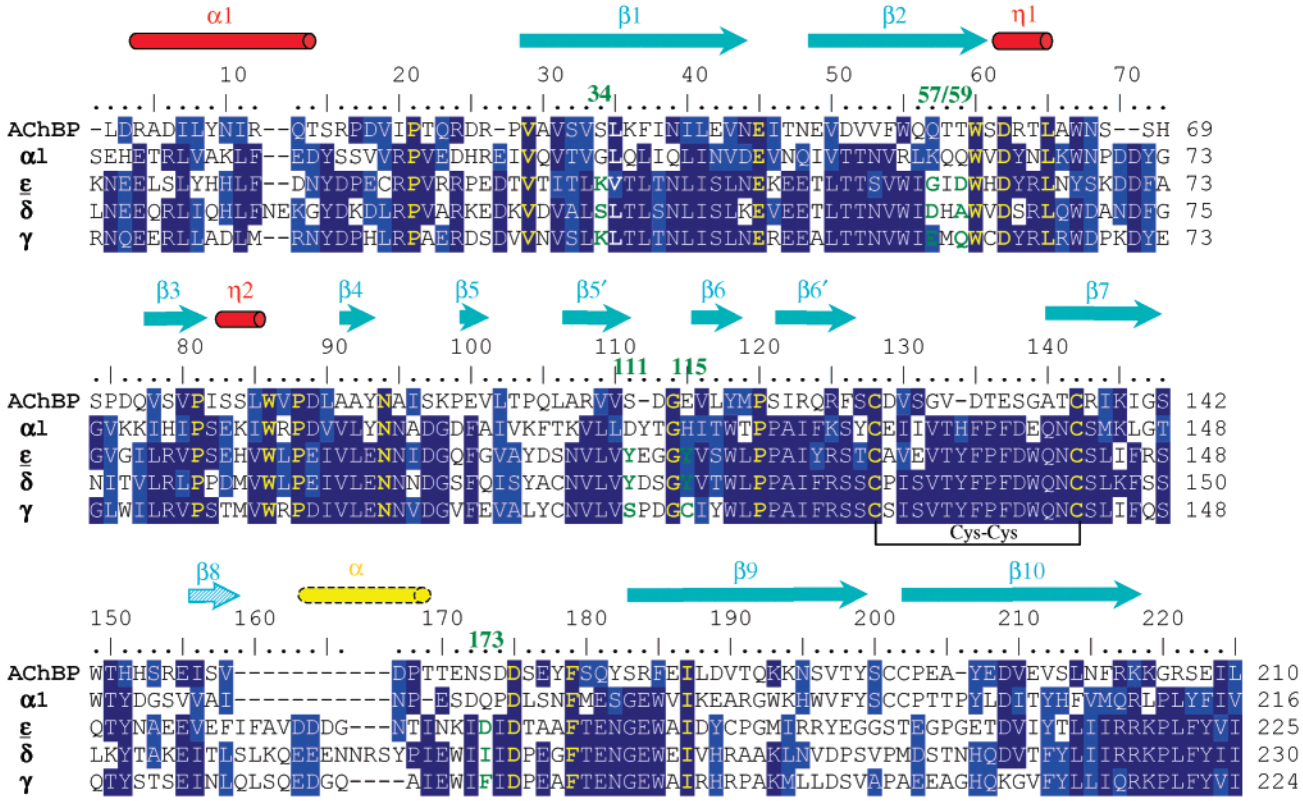

FIGURE 1: Multiple alignment of the acetylcholine binding protein (AChBP) with the α, ϵ, δ, and γ subunits of the muscle nicotinic acetylcholine receptor. Highlighting in dark blue indicates identity and light blue similarity in at least three of the five sequences. Gold-lettered residues are conserved in all five sequences. Numbers above the sequences are for the ϵ subunit, with the green numbers indicating the selectivity-determining residues. The regions of AChBP secondary structure (*4*) are indicated above the numbers, with α and 3_{10} (labeled η) helices in red and β sheets in turquoise. The β8 sheet found in the AChBP, indicated with a hatched arrow, is not present in the model of the ϵ subunit shown in Figure 6. A neighboring α helix (yellow) is modeled in the insertion region between residues 158 and 167 that is not represented in the AChBP (*4*).

non-α subunits, are located between the two α subunits in the respective fetal or adult receptor, and confer very different affinities for Wtx-1, we initially studied a series of chimeras composed of portions of γ and ϵ subunits from the mouse nAChR. Each chimera was cotransfected with wild-type α, β, and δ subunits, and Wtx-1 affinity was assessed by competition against the initial rate of [^{125}I]-α-BgTx binding (Figure 2 and Table 1). Throughout the text, chimeras are named starting with the subunit source of the N-terminal sequence, followed by the position of the chimeric junction, and ending with the subunit source of the C-terminal sequence. For example, the γ74ϵ chimera contains residues 1−74 of the γ subunit spliced to residues 75−473 of the ϵ subunit. The γ74ϵ chimera reduced affinity 82-fold compared to that of the wild-type ϵ subunit, indicating one or more determinants of selectivity are located within the first 74 residues. The γ103ϵ chimera yielded essentially the same reduction in affinity as γ74ϵ, suggesting no additional determinants between positions 74 and 103. The γ117ϵ chimera replicated the low affinity conferred by the γ subunit, giving a monophasic competition curve and a K_D of 28 μM. These results suggest that residues conferring the affinity difference between γ and ϵ subunits are located within the first 117 residues of the subunit.

However, the γ165ϵ and γ171ϵ chimeras further altered Wtx-1 affinity; γ165ϵ increased affinity 3-fold compared to that of γ117ϵ, whereas γ177ϵ decreased affinity to mimic the low-affinity characteristic of the wild-type γ subunit. The ϵ65γ76ϵ chimera gave an affinity identical to that of wild-type ϵ, indicating that this intervening γ sequence does not contribute to Wtx-1 selectivity. The collective results indicate that determinants for the γ−ϵ affinity difference localize to three regions of the subunit: residues 1−65, 103−117, and 171−177.

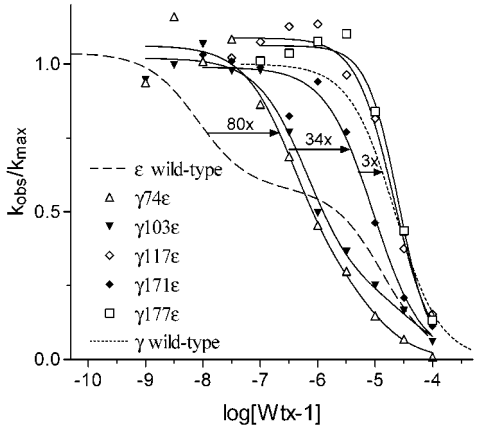

FIGURE 2: Waglerin-1 competition with the initial rate of [^{125}I]-αBgTx association for a series of γ−ϵ subunit chimeras. Chimeric subunits were constructed with the N-terminal portion of the γ subunit and the C-terminal portion from the ϵ subunit joined at the given junction point (see Experimental Procedures for a description of the chimeras). Each chimera was cotransfected with wild-type α, β, and δ subunits. k_{obs} is the observed first-order association rate constant for [^{125}I]-α-BgTx in the presence of the given concentration of waglerin-1, and k_{max} is the association rate constant in the absence of waglerin-1.

Table 1: Dissociation Constants for Wtx-1 Binding to Receptors with Chimeric $\gamma-\epsilon$ Subunits[a]

tested subunit	K_{D1} (nM)	K_{D2} (μM)	K_{D2}/K_{D1}	n_H	ΔK_{D1} (ϵ wt)	ΔK_{D1} (γ wt)	n
ϵ	9.8	20.4	2100	–	–	3700	26
γ	36000	–	–	1.2	3700	–	7
γ74ϵ	810	22.7	34	–	82	44	3
ϵ65γ76ϵ	14.8	12.7	860	–	1.5	2400	1
γ103ϵ	825	31.7	38	–	84	44	2
γ117ϵ	28200	–	–	1.2	2900	1.3	2
ϵ110γ114ϵ	134	26.8	200	–	14	1.3	2
γ165ϵ	11400	–	–	1.1	1200	3.2	1
γ171ϵ	9300	–	–	1.0	950	3.9	3
γ177ϵ	37000	–	–	1.7	3800	1.0	2
ϵ^b	6.0	10.9	1820	–	–	–	4
ϵ56γ61ϵ^b	218	11.9	55	–	36	1.1	3
ϵ57γ61ϵ^b	4.1	6.0	1460	–	0.7	0.6	1
ϵ58γ61ϵ^b	13.6	5.9	430	–	2.3	0.5	2

[a] All experiments were performed on cells transfected with mouse wild-type α, β, and δ subunits and the given γ or ϵ subunit construct. K_{D1} is the high-affinity site dissociation constant, K_{D2} the lower-affinity site dissociation constant (when the two sites have the same affinity, they are reported as K_{D1}), n_H the Hill slope for constructs in which the nonlinear regression curve fit best to a one-site analysis, ΔK_{D1} (ϵ wt) the fold difference in affinity between the K_{D1} for the tested subunit and the K_{D1} value for the ϵ wild-type subunit, ΔK_{D1} (γ wt) the fold difference in affinity between the K_{D1} with the tested subunit and the K_{D1} value with the wild-type γ subunit, and n the number of experiments. [b] Indicates experiments performed with Wtx-1 peptide amidated at C-terminus. Wtx-1-amide has ~2-fold higher affinity at both sites than wild-type Wtx-1.

Previous work identified two regions containing determinants of ligand selectivity N-terminal to position 65. One region contains K34 in the γ subunit and the equivalent S36 in the δ subunit, which contribute to binding site selectivity for carbamylcholine (*25*) and α-conotoxin MI for fetal nAChR (*13*). However, because Lys is present at position 34 in both γ and ϵ subunits, it cannot contribute to Wtx-1 selectivity for these subunits. We therefore examined the second N-terminal region (*15*), between residues 55 and 60 of the ϵ subunit, using the ϵ56γ61ϵ, ϵ57γ61ϵ, and ϵ58γ61ϵ chimeras and the H61C point mutant. The ϵ56γ61ϵ chimera reduces affinity 40-fold compared to that of the wild-type ϵ subunit, implicating residues 57−61 in the ϵ subunit and corresponding residues in the γ subunit as sources of Wtx-1 selectivity (Table 1).

To pinpoint selectivity determinants in the region of residues 56−61, we examined point mutations. The ϵG57E point mutation reduced affinity 13-fold, and ϵD59Q reduced affinity 5-fold compared to that of the wild-type ϵ subunit (Figure 3 and Table 2). Placing the two mutations in the same construct (ϵG57E/D59Q) reduced affinity 76-fold, which is essentially the same as the 80-fold reduction found for the γ74ϵ and γ103ϵ chimeras, but greater than the 40-fold reduction observed for the ϵ56γ61ϵ chimera. Thus, determinants in the N-terminal 74 amino acids are located at positions 57 and 59.

If the protein scaffolds of the γ and ϵ subunits are superimposable, increases in affinity due to mutations in the ϵ subunit should be comparable in magnitude to the decreases in affinity for equivalent mutations in the γ subunit. The point mutations γE57G, γQ59D, and γE57G/Q59D increased affinity only 2-, 2-, and 5-fold, respectively, values not nearly as large as the reductions in affinity caused by the corresponding mutations in the ϵ subunit (Figure 3 and Table 2).

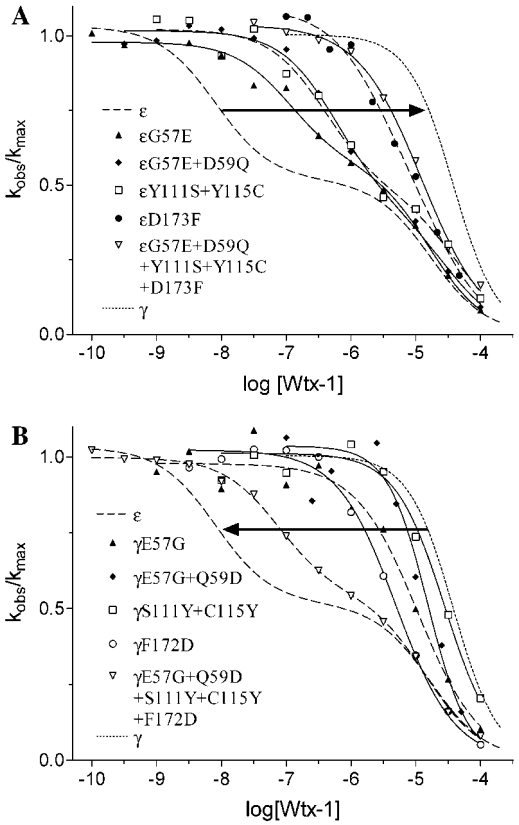

FIGURE 3: Waglerin competition with the initial rate of [^{125}I]-α-bungarotoxin binding for a series of residues determining ϵ and γ subunit selectivity. All experiments were performed on HEK cells cotransfected with wild-type α, β, and δ subunits and the indicated mutated ϵ or γ subunit. Sequence analysis is depicted in detail in Figure 1. Arrows indicate the direction of shift in the binding curve resulting from the given mutation. Waglerin K_D values for each receptor are given in Table 2. (A) ϵ to γ subunit point mutations. Residues in the ϵ subunit template were mutated at the selectivity-determining residues to the corresponding amino acids found in the γ subunit. (B) γ to ϵ subunit point mutations. Residues in the γ subunit template were mutated at the selectivity-determining residues to the corresponding amino acids found in the ϵ subunit.

This difference between ϵ and γ subunits following mutation suggests the presence of additional selectivity determinants in the N-terminus of the subunit that either interact with residues at positions 57 and 59 or position Wtx-1 to interact with these determinants.

To localize selectivity determinants within the second N-terminal region, residues 103−117, three $\epsilon-\gamma-\epsilon$ chimeras were made: ϵ110γ117ϵ, ϵ110γ114ϵ, and ϵ114γ117ϵ. Following cotransfection with complementary wild-type subunits, only the ϵ110γ114ϵ chimera was expressed well, and it reduced affinity 23-fold relative to that of the wild-type ϵ subunit (Table 1), indicating key determinants between positions 110 and 114. The residue at position 111 is a key selectivity determinant for α-conotoxin MI at the $\alpha-\gamma$ site in fetal AChR (*13*), and is Tyr in the ϵ subunit and Ser in the γ subunit. The point mutant ϵY111S reduced Wtx-1 affinity 4-fold, and ϵY115C, which replicates the position 115 difference between ϵ and γ subunits (Figure 1), reduced affinity 13-fold. The double mutation ϵY111S/Y115C reduced affinity 30-fold (Figure 3A and Table 2), close to the additive change in affinity for individual point mutants, and nearly identical to the difference in affinity between the γ103ϵ and γ117ϵ chimeras. Thus results from chimeras and

Table 2: Dissociation Constants for the nAChR with γ or ϵ Residue Substitutions into ϵ or γ Subunits, Respectively[a]

γ subunit substitutions into an ϵ subunit template	$K_{D\alpha-\epsilon}$ (nM)	$K_{D\alpha-\delta}$ (μM)	$K_{D\alpha-\epsilon}/K_{D\alpha-\delta}$	n_H	$\Delta K_{D\alpha-\epsilon}$	n
ϵ	9.8	20.4	2100	−	−	26
ϵG57E	125	18.0	140	−	13	3
ϵD59Q	47	33.9	720	−	5	3
ϵG57E/D59Q	743	34.8	47	−	76	2
ϵY111S	38	23.2	610	−	4	2
ϵY115C	126	14.7	120	−	13	3
ϵY111S/Y115C	290	27.4	94	−	30	3
ϵD173F	2710	23.9	9	−	280	3
ϵY111S/D173F	8900	−	−	1.0	910	1
ϵG57E/D173F	13800	−	−	1.0	1400	3
ϵG57E/D59Q/D173F	17900	−	−	1.0	1800	2
ϵG57E/D59Q/Y111S/Y115C/D173F	11500	−	−	1.1	1200	2
ϵ subunit substitutions into a γ subunit template	**$K_{D\alpha-\gamma}$ (nM)**	**$K_{D\alpha-\delta}$ (μM)**	**$K_{D\alpha-\gamma}/K_{D\alpha-\delta}$**	**n_H**	**$\Delta K_{D\alpha-\gamma}$**	**n**
γ	36000	−	−	1.2	−	7
γE57G	14700	−	−	1.0	2.5	2
γQ59D	11400	−	−	1.2	3	3
γE57G/Q59D	9200	−	−	1.2	5	3
γC61H	27400	−	−	1.1	1.3	1
γQ59D/C61H	7700	−	−	0.9	5	1
γS111Y	20800	−	−	1.2	1.7	2
γC115Y	20700	−	−	1.1	1.7	2
γS111Y/C115Y	26900	−	−	1.5	1.3	2
γE57G/C115Y	18200	−	−	1.0	2.0	2
γF172D	7200	−	−	0.9	5	3
γE57G/F172D	537	29.2	94	−	67	3
γS111Y/F172D	2510	22.2	9	−	14	1
γE57G/Q59D/F172D	525	29.8	57	−	68	3
γE57G/C115Y/F172D	407	28.4	70	−	88	3
γE57G/Q59D/S111Y/C115Y	15300	−	−	1.0	2	2
γE57G/Q59D/S111Y/C115Y/F172D	98.3	16.6	170	−	370	3

[a] All experiments performed on cells transfected with mouse wild-type α, β, and δ subunits and the given ϵ or γ subunit. $K_{D\alpha-\epsilon}$, $\alpha-\epsilon$ site K_D; $K_{D\alpha-\delta}$, $\alpha-\delta$ site K_D; $\Delta K_{D\alpha-\epsilon/\gamma}$, fold change in the mutant $K_{D\alpha-\epsilon/\gamma}$ value compared to the wild-type $K_{D\alpha-\epsilon}$ ($\Delta K_{D\alpha-\delta}$ values differed by less than 2-fold from wild-type $K_{D\alpha-\delta}$); n, number of experiments. Results of experiments in which mutation of the ϵ or γ site yielded a $K_{D\alpha-\epsilon/\gamma}$ which superimposed on $K_{D\alpha-\delta}$ are listed in the $K_{D\alpha-\epsilon/\gamma}$ column only, though this value represents the composite Wtx-1 K_D found at both the $\alpha-\epsilon/\gamma$ and $\alpha-\delta$ sites.

point mutants indicate residues at positions 111 and 115 are determinants of Wtx-1 selectivity.

The γ117ϵ chimera reduced Wtx-1 affinity to nearly that conferred by the wild-type γ subunit, and the four identified determinants, two major (Gly-57 and Tyr-115) and two minor (Asp-59 and Tyr-111), all lie within this N-terminal 117-amino acid region. Although the quadruple mutant of these determinants was not made in the ϵ subunit, the sum of the respective affinity reductions for the four mutants fully accounts for the entire 3700-fold difference in affinity between $\alpha-\epsilon$ and $\alpha-\gamma$ binding sites, as well as that between $\alpha-\epsilon$ and $\alpha-\gamma$117ϵ sites. We therefore concluded that these four determinants account fully for Wtx-1 selectivity between $\alpha-\epsilon$ and $\alpha-\gamma$ binding sites. However, as seen with the γE57G and γQ59D mutants, the γS111Y and γC115Y mutants did not significantly increase Wtx-1 affinity relative to that of the wild-type γ subunit (Table 2). Furthermore, Wtx-1 affinity conferred by the quadruple mutant, γE57G/Q59D/S111Y/C115Y, did not change compared to that of the wild-type γ subunit (Table 2). Hence, within the N-terminal region containing residues 1−117, a large convergence of affinities between ϵ and γ can only be achieved by γ substitutions in the ϵ template, which reduces affinity, but not by ϵ substitutions in the γ template. Accordingly, we sought additional determinants of Wtx-1 affinity, and examined whether they affect contributions of the four identified selectivity determinants.

The γ165ϵ and γ171ϵ chimeras increased affinity 3-fold compared to those of γ117ϵ, γ177ϵ, or wild-type γ (Table 1), suggesting a minor determinant between positions 171 and 177. This region harbors a second determinant of α-conotoxin MI selectivity, γPhe-172/ϵAsp-173/δIle-178 (*13*). Paradoxically, the ϵD173F point mutant, far outside the N-terminal 117-amino acid region thought to harbor most of the selectivity determinants, diminished affinity by 280-fold. This unexpected reduction in affinity is significantly greater than for any individual point mutation studied thus far, far greater than the 4-fold affinity change between the γ171ϵ and γ177ϵ chimeras. Analogously, the 5-fold increase in affinity observed for the homologous residue replacement in the γ subunit, γF172D (Figure 3B and Table 2), while consistent with the small affinity difference between the γ173ϵ and γ177ϵ chimeras, was far smaller than the 276-fold decrease in affinity for the converse residue replacement in the ϵ subunit, ϵD173F.

The $\gamma-\epsilon$ chimeras and single point mutations reveal three regions of primary sequence that determine the high affinity of waglerin-1 for the $\alpha-\epsilon$ versus the $\alpha-\gamma$ site: (a) N-terminus to position 74, (b) between positions 103 and 117, and (c) between positions 171 and 177. When the ϵ subunit is mutated at positions 57, 59, 111, 115, and 173 to the corresponding residues in γ, the individual reductions in affinity fully account for the corresponding reductions suggested by the chimeras. When these five mutations were

Table 3: Waglerin-1 Dissociation Constants for δ Subunit Substitutions into an ϵ Subunit and with ϵ−δ Chimeras[a]

δ subunit substitutions into an ϵ subunit template	$K_{D\alpha-\epsilon}$ (nM)	$K_{D\alpha-\delta}$ (μM)	$K_{D\alpha-\delta}/K_{D\alpha-\epsilon}$	$\Delta K_{D\alpha-\epsilon}$	*n*
ϵ	9.8	20.4	2100	−	26
ϵK34S	55.3	33.0	600	6	2
ϵG57D	288	26.9	93	29	3
ϵD59A	10.8	18.1	17000	1	2
ϵG57D/D59A	77.0	22.4	290	8	2
ϵD173I	1040	22.9	22	106	3
ϵK34S/D173I	360	25.3	70	37	3
ϵG57D/D173I	625	29.3	47	64	3
ϵG57D/D59A/D173I	1200	42.5	35	120	2
ϵK34S/G57D/D59A/D173I	1970	61.7	31	200	3

ϵ−δ chimeras and ϵ substitutions into a δ subunit template	$K_{D\alpha-\epsilon}$ (nM)	$K_{D\alpha-\delta}$ (μM)	$K_{D\alpha-\delta}/K_{D\alpha-\epsilon}$	$\Delta K_{D\alpha-\delta}$	*n*
δI178D	18.7	3.0	160	7	7
ϵ117δ	16.6	4.0	240	5	3
δD114E/I178D	23.4	2.2	95	9	2
δS115G/I178D	14.0	2.3	160	9	2
δT119S/I178D	18.5	1.2	67	17	3
δD114E/S115G/T119S	7.1	5.9	830	4	2
δD114E/S115G/T119S/I178D	4.8	2.5	760	8	2
ϵ117δI178D	12.1	0.12	10	170	2
ϵ65δ	32.3	6.9	210	3	5
ϵ65δI178D	23.2	0.13	6	160	5
δ31ϵ65δI178D	5.8	0.24	41	84	2

[a] The top section lists results of experiments performed on cells transfected with wild-type α, β, and δ subunits and the given ϵ subunit. The bottom section lists results of experiments performed on cells transfected with wild-type α, β, and ϵ subunits and the given δ subunit chimera and/or substitution. Column labels are as defined in Table 2.

incorporated into a single ϵ subunit, the affinity decreased to within 3-fold of that of the wild-type γ subunit (Figure 3A and Table 2). Conversely, whereas mutation of these same residues *individually* in the γ subunit fell far short of the high affinity expected for the wild-type α−ϵ site, the corresponding quintuple mutant in the γ subunit, γE57G/Q59D/S111Y/C115Y/F172D, increased Wtx-1 affinity to within 10-fold of that of the wild-type α−ϵ site (Table 2 and Figure 3B). Thus, the collective results delineate multiple determinants of Wtx-1 selectivity in ϵ and γ subunits and, moreover, show that their contributions are interdependent. This interdependence of residues is analyzed in the Discussion.

δ-ϵ Subunit Determinants for Waglerin-1. Wtx-1 selects between α−ϵ and α−δ sites in the adult nAChR by 2100-fold because of different contributions of ϵ and δ subunits. Although the δ and ϵ subunits exhibit less residue identity than the γ and ϵ subunits and occupy different positions in the ordering of the subunits around the pentamer, we tested the hypothesis that residues at equivalent positions of these subunits govern Wtx-1 selectivity for sites in the adult nAChR. We constructed chimeras and point mutants based on the δ subunit, cotransfected them with wild-type α, β, and ϵ subunits, and assessed Wtx-1 binding. To test the contribution of the N-terminal region, we examined the ϵ65δ chimera, but found only a 3-fold increase in affinity compared to that of wild-type δ. Point mutations of the identified γ/ϵ determinants, δD59G and δA61D, failed to increase affinity. The converse mutation in the ϵ subunit, ϵG57D, decreased affinity 29-fold, whereas the ϵD59A mutant was without effect (Table 3). Thus, as observed for mutations in γ and ϵ subunits, mutation of residue 59 in the δ subunit had a markedly different consequence than mutation of the equivalent residue in the ϵ subunit, again suggesting multiple residues interact to confer Wtx-1 selectivity.

The ϵD173F mutation, which substitutes the residue at the equivalent position in the γ subunit, reduces affinity by 280-fold, the largest reduction for any single-residue change (Table 2). The corresponding ϵ to δ mutation, ϵD173I, reduces affinity by 106-fold, but the converse δ to ϵ mutation, δI178D, increases affinity only 7-fold (Table 3). These results provide additional evidence that multiple residues interact to confer Wtx-1 selectivity for sites in the adult nAChR. Thus, subsequent mutations were made in a construct containing the δI178D mutation to investigate cooperative interactions.

We initially combined the ϵ65δ chimera with the δI178D point mutant to give ϵ65δ/I178D. This construct increased affinity 156-fold compared to that of wild-type δ (Table 3), which is far greater than the 21-fold increase expected from additive contributions (3-fold for ϵ65δ and 7-fold for δI178D). Hence, one or more residues N-terminal to position 65 appear to be energetically coupled to δI178. Additional constructs, ϵ117δ and ϵ117δ/I178D, gave affinities essentially identical to those of the ϵ65δ and ϵ65δ/I178D constructs, respectively (Table 3), suggesting that no additional ϵ/δ selectivity determinants are present between positions 67 and 119 of the δ subunit.

To test further for interacting residues, we started with the mutation δI178D and introduced a series of δ to ϵ subunit mutations at the following single sites: δD59G, δA61D (Table 5), δH60I, δV63H, and δS65Y. No evidence for interacting residues was obtained for any of these double mutants, although the ϵD59G/I178D mutation increased affinity 3-fold compared to that of the δI178D mutation alone. The triple mutation δD57G/A61D/I178D increased affinity 46-fold compared to that of wild-type δ (Table 5), the largest increase of any combination of point mutants in the δ subunit.

Only one other determinant of ligand selectivity N-terminal to position 55 has been described: Lys-34 in γ and ϵ subunits and the equivalent Ser-36 in the δ subunit (*13*, *25*). The point mutant ϵK34S reduced affinity for Wtx-1 by almost 6-fold (Table 3), but the converse mutant δS36K mutant paradoxically *reduced* affinity by 2-fold. By comparison, the δS36K/I178D double mutant enhanced affinity 4-, 60-, and 30-fold over those of the δI178D mutant, the δS36K mutant, and the wild-type δ subunit, respectively. That δS36K enhances rather than reduces affinity when combined with δI178D indicates that these two oppositely charged residues interact in contributing to Wtx-1 selectivity.

To look further for ϵ/δ selectivity determinants, we examined the three residues that differ between positions 113 and 119 of the δ subunit, as two residues in this region contribute to the ϵ/γ selectivity difference for Wtx-1. We mutated δD114, δS115, and δT119 to the corresponding residues in the ϵ subunit and combined each with the δI178D mutant. For all three double mutations, no change in affinity was observed compared to that of δI178D alone (Table 3). The triple mutant, δD114E/S115G/T119S, increased affinity 3-fold, but this increase was not maintained in the δD114E/

Table 4: Pairwise Interaction Energies (Linkages) for Multiple Mutations in the ϵ and γ Subunit Templates[a]

ϵ subunit template	mut1	mut2	Ω	$\Delta\Delta G_{INT}$ (kcal/mol)
ϵ to δ mutations				
G57D/D59A	G57D	D59A	4.1	−0.84
K34S/D173I	K34S	D173I	**16.3**	**−1.65**
G57D/D173I	G57D	D173I	**48.8**	**−2.29**
G57D/D59A/D173I	G57D/D59A	D173I	6.8	−1.13
G57D/D59A/D173I	G57D/D173I	D59A	1.7	0.33
K34S/G57D/D59A/D173I	G57D/D59A/D173I	K34S	3.4	−0.73
K34S/G57D/D59A/D173I	G57D/D59A	K34S/D173I	1.4	−0.21
ϵ to γ mutations				
G57E/D59Q	G57E	D59Q	1.2	0.13
Y111S/Y115C	Y111S	Y115C	1.7	−0.30
G57E/D173F	G57E	D173F	2.5	−0.54
G57E/D59Q/D173F	G57E/D173F	D59Q	3.7	−0.77
G57E/D59Q/D173F	G57E/D59Q	D173F	**11.5**	**−1.44**
G57E/D59Q/ Y111S/Y115C/D173F	G57E/D59Q/D173F	Y111S/Y115C	**46.1**	**−2.26**

γ subunit template	mut1	mut2	Ω	$\Delta\Delta G_{INT}$ (kcal/mol)
γ to ϵ mutations				
E57G/Q59D	E57G	Q59D	2.2	0.46
S111Y/C115Y	S111Y	C115Y	2.2	0.48
E57G/C115Y	E57G	C115Y	2.2	0.45
E57G/F172D	E57G	F172D	5.5	−1.00
E57G/Q59D/F172D	E57G/Q59D	F172D	3.5	−0.74
E57G/Q59D/F172D	E57G/F172D	Q59D	3.4	0.72
E57G/C115Y/F172D	E57G/F172D	C115Y	1.3	0.16
E57G/C115Y/F172D	E57G/C115Y	F172D	**9.0**	**−1.29**
E57G/Q59D/C115Y	E57G/Q59D	C115Y	2.2	0.47
E57G/Q59D/S111Y/C115Y/F172D	E57G/Q59D/F172D	S111Y/C115Y	4.0	−0.82
E57G/Q59D/S111Y/C115Y/F172D	E57G/Q59D/S111Y/C115Y	F172D	**31.2**	**−2.03**

[a] All experiments were performed on cells transfected with mouse wild-type α, β, and δ subunits and the given ϵ (top section) or γ (bottom section) subunit mutation(s). Actual K_D values are given in Tables 2 and 3. mut1 and mut2 are the mutation(s) represented in Scheme 1 of the text. Ω is defined in eq 2 of the text, and its reciprocal is shown for values <1. $\Delta\Delta G_{INT}$ is defined in eqs 3 and 4 of the text. Bold numbers indicate $|\Delta\Delta G_{INT}| \geq 1.3$ kcal/mol.

Table 5: δ Subunit Mutation Interaction Energies[a]

mut1		mut2		mut1 and mut2			
mutation(s)	$K_{D\alpha-\delta}$ (μM)	mutation(s)	$K_{D\alpha-\delta}$ (μM)	mutations	$K_{D\alpha-\delta}$ (μM)	Ω	$\Delta\Delta G_{INT}$ (kcal/mol)
D59G	19.9	A61D	14.4	δD59G/A61D	6.0	2.5	−0.54
S36K	41.6	D59G/A61D	6.0	δS36K/D59G/A61D	21.3	1.7	0.33
S36K	41.6	I178D	3.0	δS36K/I178D	0.68	**8.9**	**−1.29**
D59G	19.9	I178D	3.0	δD59G/I178D	1.0	3.1	−0.66
A61D	14.4	I178D	3.0	δA61D/I178D	2.9	1.4	0.18
D59G	19.9	A61D/I178D	2.9	δD59G/A61D/I178D	0.44	6.7	−1.12
A61D	14.4	D59G/I178D	1.0	δD59G/A61D/I178D	0.44	1.6	−0.28
I178D	3.0	D59G/A61D	1.0	δD59G/A61D/I178D	0.44	2.0	−0.40
S36K	41.6	D59G/I178D	1.0	δS36K/D59G/I178D	2.3	1.1	0.06
D59G	19.9	S36K/I178D	0.68	δS36K/D59G/I178D	2.3	3.2	0.69
S36K	41.6	A61D/I178D	2.9	δS36K/A61D/I178D	0.53	**11.0**	**−1.41**
A61D	14.4	S36K/I178D	0.68	δS36K/A61D/I178D	0.53	1.1	0.06
S36K	41.6	D59G/A61D/I178D	0.44	δS36K/D59G/A61D/I178D	0.14	6.6	−1.11
D59G	19.9	S36K/A61D/I178D	0.53	δS36K/D59G/A61D/I178D	0.14	4.0	−0.82
A61D	14.4	S36K/D59G/I178D	2.3	δS36K/D59G/A61D/I178D	0.14	**11.7**	**−1.45**
I178D	3.0	S36K/D59G/A61D	21.3	δS36K/D59G/A61D/I178D	0.14	**22.5**	**−1.84**
D59G/A61D	6.0	S36K/I178D	0.68	δS36K/D59G/A61D/I178D	0.14	1.1	−0.07

[a] All experiments were performed on cells transfected with mouse wild-type α, β, and ϵ subunits and the given mutated δ subunit. The columns mut1 and mut 2 list the mutated δ subunit constructs represented by each pathway of the thermodynamic cycle described in Scheme 1 of the text. The column "mut1 and mut2" lists experimentally determined K_D values for the combined mutations. Ω is defined in eq 2 of the text, and its reciprocal is shown for values <1. $\Delta\Delta G_{INT}$ is defined in eqs 3 and 4 of the text. Bold numbers indicate significant $\Delta\Delta G_{INT}$ values of ≥1.3 kcal/mol. The $K_{D\alpha-\delta}$ value for the wild-type receptor is given in Table 2.

S115G/T119S/I178D quadruple mutant (Table 3). Hence, residues between positions 113 and 119 of the δ subunit do not contribute to Wtx-1 selectivity, unlike residues in equivalent positions in ϵ and γ subunits.

Finally, we placed into a single construct mutations at the four positions that contribute to Wtx-1 selectivity between α−ϵ and α−δ sites. The δS36K/D59G/A61D/I178D mutant increases affinity 150-fold compared to that of mouse wild-type δ, or to within 14-fold of the affinity of the wild-type α−ϵ site. The K_D for this quadruple mutant is comparable to those for the following chimeras combined with point mutations: δ31ϵ65δ/I178D, ϵ65δ/I178D. and ϵ117δ/I178D.

Thus, Wtx-1 selectivity for α−ϵ over α−δ sites arises from differences in equivalent residues at three of four positions that confer selectivity for α−ϵ over α−γ sites.

DISCUSSION

The waglerin family of peptides are the only toxins from the Viperidae family of snakes known to block neuromuscular transmission by interacting with the nAChR. As such, they possess several features that should prove to be useful in understanding functional antagonism and the structure of nicotinic receptors. First, as 22−24-amino acid peptides with a single disulfide bond, their primary and tertiary structures are unique to the known peptidic antagonists (*26*, *27*). Second, they show unusual specificity in antagonism at the receptor for certain animal species, with a preference for mouse over rat (*10*, *28*), human (*10*), and chick (*29*). Third, the resistance of the immature mouse to waglerin toxins (*30*) and the expression of the ϵ subunit in place of γ during maturation of the neuromuscular junction (*31*, *32*) indicate that subunit replacement accounts for the different sensitivities to Wtx-1. In vitro, Wtx-1 binding at the α−ϵ subunit interface shows a 2000-fold enhancement of affinity over the α−δ (*10*) and α−γ counterparts.

The initial goal of the experiments presented here was to delineate the residues in the non-α subunits mediating this 2000-fold selectivity of Wtx-1 for the α−ϵ binding site compared to the α−δ and α−γ sites of the muscle nAChR. In the course of performing these experiments, we found that multiple mutations often gave results dramatically different from those expected from the sum of the contributions of the single mutants. This led us to analyze intrasubunit linkages by thermodynamic mutant cycle analysis (*33*).

Residues Mediating Wtx-1 Site Selectivity. The γ and ϵ subunits are located between the two α subunits in the respective fetal or adult receptor, but confer very different affinities for Wtx-1. Substitution of the five determinants from the γ subunit into the ϵ subunit yields an assembled receptor with reduced affinity approximating that of the α−γ site (Figure 3A). Conversely, substitution of the same five residues from the ϵ subunit (residues 57, 59, 111, 115, and 173) into the γ subunit increases affinity to within 10-fold of that of the α−ϵ site (Figure 3B). The δ subunit occupies a position different from those of γ and ϵ in the receptor pentamer and is more distant from either in sequence homology (Figure 1). Nevertheless, we interchanged the four selectivity determinants between δ and ϵ subunits (residues 34, 57, 59, and 173), and replicated the low affinity conferred by δ in the ϵ subunit and, conversely, approached within 14-fold the high affinity conferred by ϵ in the δ subunit.

We were not able to replicate completely the α−ϵ site affinity with mutations in either the γ or δ subunit. This suggests additional unidentified residues contribute to Wtx-1 selectivity, or that the scaffolds of the ϵ, γ, and δ subunits are not identical. However, our data, as well as previously recorded data, support the concept of similar but not identical scaffolds of these non-α subunits. A majority of the site selectivity displayed by several different ligands can be ascribed to mutations at aligned positions of the subunits that both *decrease* affinity at the high-affinity binding site and *increase* affinity at the low-affinity site (*11*, *13*, *14*, *34*), strongly suggesting that these mutations do not alter affinity through nonspecific mechanisms. Our inability to completely replicate high-affinity binding at the α−γ and α−δ sites likely results from subtle variations among the many nonidentical residues in the non-α subunits, in addition to inserted or deleted residues (Figure 1). Such multiple structural differences would be very difficult to replicate in a mutated construct. Thus, our study identifies the principal determinants of Wtx-1 selectivity.

Of the six residues defining Wtx-1 binding site selectivity, three contribute to selectivity of the α−ϵ over both α−γ and α−δ sites (residues 57, 59, and 173), two are unique to selectivity of α−ϵ over α−γ sites (residues 111 and 115), and one is unique to selectivity of α−ϵ over α−δ sites (residue 36). Residues at these aligned positions have also been identified as determinants of α-conotoxin MI (*13*), carbamylcholine (*25*), and D-tubocurarine (*11*, *15*) selectivity. Neighboring residues ϵPro176 and ϵGlu177 mediate selectivity of NmmI, a three-fingered α-neurotoxin of 62 residues (*14*, *35*). What appears to be unique to Wtx-1 selectivity is the principal dependence on Asp-173 in governing the specificity conferred by the other five residues. The sections below analyze the intrasubunit residue interactions responsible for Wtx-1 selectivity.

Intrasubunit Linkages in the Binding Site. In a fashion analogous to investigating a complex between two molecules, pairwise interactions between residues within a subunit can be analyzed using thermodynamic mutant cycle analysis (*33*, *35*−*39*). The free energy change associated with ligand binding can be computed for the mutated and wild-type receptor, with the change in Δ*G* upon mutation given by

$$\Delta\Delta G = RT \ln \frac{K_{\mathrm{Dmut}}}{K_{\mathrm{Dwt}}} \qquad (1)$$

A reversible reaction characterized by a cyclic reaction scheme requires microscopic reversibility. In this case, two mutations in an individual receptor ($R_{mut1,mut2}$) subunit are compared to the wild-type receptor ($R_{wt,wt}$) and the two single mutants by the following thermodynamic cycle:

Scheme 1

$$\begin{array}{ccc} R_{wt,wt} & \leftrightarrows & R_{wt,mut2} \\ \downarrow\uparrow & & \downarrow\uparrow \\ R_{mut1,wt} & \leftrightarrows & R_{mut1,mut2} \end{array}$$

For each of the R mutation states of the receptor indicated in Scheme 1, a free energy change of waglerin-1 binding (Δ*G*°) can be determined. If the individual mutations contribute independently to the binding site for Wtx-1, the total Δ*G* for the series of hypothetical binding reactions from any state of the cycle back to the starting state should equal zero. If the interaction energy is less than or greater than the additive value, then it suggests the two individual mutations are energetically coupled with each other, and mutually interact in contributing to Wtx-1 binding. The equations are derived as follows:

$$\Omega = \frac{K_{\mathrm{Dmut1,mut2}} K_{\mathrm{Dwt,wt}}}{K_{\mathrm{Dmut1,wt}} K_{\mathrm{Dwt,mut2}}} \quad (2)$$

$$\Delta\Delta G_{\mathrm{INT}} = RT \ln \Omega \quad (3)$$

$$= RT \ln K_{\mathrm{Dmut1,mut2}} - RT \ln K_{\mathrm{Dmut1,wt}} - RT \ln K_{\mathrm{Dwt,mut2}} + RT \ln K_{\mathrm{Dwt,wt}}$$

$$= \Delta G^{\circ}_{\mathrm{mut1,mut2}} - \Delta G^{\circ}_{\mathrm{mut1,wt}} - (\Delta G^{\circ}_{\mathrm{wt,mut2}} - \Delta G^{\circ}_{\mathrm{wt,wt}}) \quad (4)$$

Using mutant cycle analysis, Wtx-1 binding to receptors with multiple mutations can be compared to the binding to receptors with single mutations to determine their degree of interaction. Tables 4 and 5 summarize the data for the groups of mutations described in the following sections. A negative $\Delta\Delta G_{\mathrm{INT}}$ value represents a higher affinity (lower K_{D} value) for the double (or multiple) mutant than the sum of single mutants, whereas a positive value represents a lower affinity (greater K_{D} value) than the sum of the single mutants.

Intrasubunit Interactions Revealed by Interchange of γ and ϵ Residues. The ϵD173F mutation reduced affinity more than any single mutation in the ϵ subunit. When ϵD173F is combined with ϵG57E or the double mutation ϵG57E/D59Q, the resultant ϵ subunit shows a less than additive reduction of $\Delta\Delta G$ (Figure 3), making these three residues likely candidates for interaction when ϵ residues are substituted into a γ subunit. The γE57G/Q59D double mutant and the γF172D mutants only increase affinity by 5-fold each. However, when the γF172D point mutant is combined with γE57G, γE57G/C115Y, and γE57G/Q59D, the interaction energies ($\Delta\Delta G_{\mathrm{INT}}$) are −1.00, −1.29, and −0.74 kcal/mol for the three combinations, respectively (Table 4), suggesting coupling between γF172 and γE57. Furthermore, there was little or no interaction between γE57G/F172D and γC115Y, again suggesting coupling between γE57 and γF172.

Results from multiple-point mutants also revealed interaction between γF172 and several residues jointly. The quadruple mutant γE57G/Q59D/C115Y/F172D was not expressed. However, the quintuple mutant γE57G/Q59D/S111Y/C115Y/F172D expressed very well and revealed an interaction energy of −2.03 kcal/mol between the γF172D mutation and the γE57G/γQ59D/γS111Y/γC115Y quadruple mutant (Figure 5 and Table 4).

The preceding data indicate two requirements for Wtx-1 selectivity. First, the high-affinity interaction of Wtx-1 with the nAChR binding sites strongly depends on the presence of an Asp residue at the ϵ-173/γ-172 position. This is supported by the fact that in the ϵ subunit, there is little additional *reduction* in affinity when the other affinity determinants are added to the ϵD173F mutant, and in the γ subunit, there is little *increase* in affinity resulting from γ to ϵ mutations at positions 57, 59, 111, and 115 *unless* the γF172D mutation (homologous with position 173 in ϵ) is present (Table 4). Second, positions 57 and 173 are most likely interdependent, as discussed further below. The data do not, however, allow us to distinguish conclusively between Asp-173 influencing the orientation of Wtx-1 in the binding site or positioning the other selectivity-determining residues within the non-α subunit.

Intrasubunit Interactions Revealed by Interchange of δ and ϵ Residues. Of the ϵ to δ point mutations, the two largest

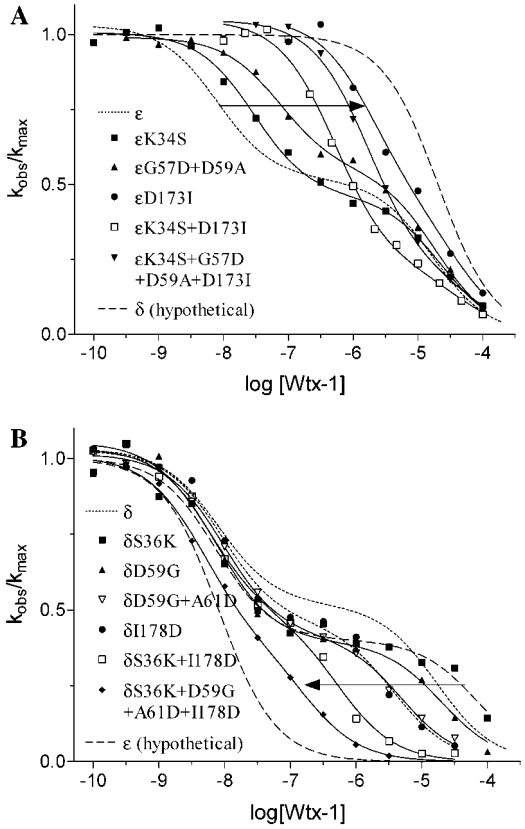

FIGURE 4: Waglerin competition with the initial rate of [^{125}I]-α-BgTx binding for a series of residues determining ϵ and δ subunit selectivity. Arrows indicate the direction of shift in the binding curve resulting from the given mutations in each graph. The analysis is described in detail in Experimental Procedures, and dissociation constants are found in Table 3. (A) ϵ to δ subunit mutations. The given point mutations were made in which the ϵ subunit residues were mutated to the amino acid found at the corresponding position of the δ subunit. The dashed line at the right of the graphs represents the hypothetical position of the δ wild-type curve analyzed as a single site. In each experiment, cells were cotransfected with wild-type α, β, δ, and given mutated ϵ subunit. (B) δ to ϵ subunit point mutations. Point mutations in the δ subunit were constructed, and cells were cotransfected with wild-type α, β, and ϵ subunits. The dashed line at left side of the graph indicates the hypothetical position of the curve if the α−δ site has the same affinity as the wild-type α−ϵ site.

reductions in affinity of 106- and 29-fold were found for ϵD173I and ϵG57D, respectively. The ϵG57D/D173I double mutant reduced affinity only slightly more than the ϵD173I mutant alone, resulting in a $\Delta\Delta G_{\mathrm{INT}}$ of −2.3 kcal/mol (Table 4). Also, residues at the ϵ-34 and ϵ-173 positions interact with each other. The ϵK34S mutant reduces affinity 6-fold, whereas the ϵK34S/D173I double mutant increases affinity 3-fold more than ϵD173I mutant by itself, yielding a $\Delta\Delta G_{\mathrm{INT}}$ of −1.65 kcal/mol (Table 4). As observed for residues interchanged between ϵ and γ subunits, the homologous position ϵ173/γ172/δ178 is critical for enhancing affinity for combinations of mutations. Of the point mutations made in the δ subunit, the δS36K mutation couples most strongly with the δI178D mutation, giving a $\Delta\Delta G_{\mathrm{INT}}$ of −1.29 kcal/mol, or nearly 1 order of magnitude of change in K_{D} (Table 5).

An even greater interaction energy for the δ mutants is achieved with δI178D when combined with δS36K/D59G/A61D; this mutant cycle yielded a $\Delta\Delta G_{\mathrm{INT}}$ of −1.84 kcal/mol (Table 5). The δS36K/D59G/A61D triple mutant confers

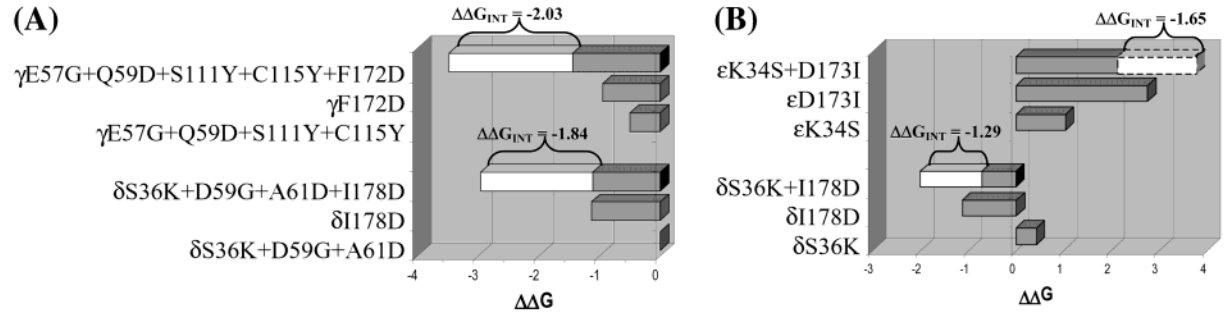

FIGURE 5: Interaction energies of combinations of mutations within a subunit. The bar graphs above demonstrate interaction energies ($\Delta\Delta G_{INT}$) occurring between homologous positions ϵ-173, δ-178, and γ-172 and the other selectivity-determining residues. All bars indicate changes in the binding free energy ($\Delta\Delta G$; see eq 1 in the text) upon mutation of the residue(s) designated to the left of the bars. The white segments of the bars represent interaction free energies ($\Delta\Delta G_{INT}$; see eq 3 in the text) between the sets of mutants in each of the groups; the actual $\Delta\Delta G_{INT}$ value is indicated with the bracket above the white bar. Negative $\Delta\Delta G$ values indicate increases in affinity compared to that of the wild type, and positive $\Delta\Delta G$ values indicate decreases in affinity. Dashed lines on white bars indicate a *subadditive* $\Delta\Delta G_{INT}$ contribution to the total $\Delta\Delta G$ for the construct, and solid lines on white bars indicate a *supra-additive* $\Delta\Delta G_{INT}$ contribution to the total $\Delta\Delta G$ for the construct. The data are given in Tables 4 and 5. (A) $\Delta\Delta G_{INT}$ values for γ-172/δ-178 mutants with the other selectivity-determining residues. (Top bars) The white bar indicates the *supra-additive increase* in affinity resulting from combining the γF172D mutation with the γE57G/Q59D/S111Y/C115Y quadruple mutant. (Bottom bars) The white bar indicates the *supra-additive increase* in affinity resulting from combining the δS36K/D59G/A61D triple mutant with the δI178D point mutation. (B) Interaction energies between residues 34/36 and 173/178 in ϵ/δ subunits. (Top bars) The mutations in the ϵ subunit indicate that positions 34 and 173 in ϵ interact with each other to facilitate binding of waglerin-1 to the receptor. The dashed white bar in the ϵK34S/D173I double mutation indicates a *sub-additive decrease* in affinity. (Bottom bars) The mutations in the δ subunit indicate that positions 36 and 178 interact with each other to facilitate binding of waglerin-1 to the receptor. In this case, the δS36K/I178D double mutation gives a *supra-additive increase* in affinity.

the same affinity as wild-type δ, while δI178D confers 7-fold higher affinity; however, the combined quadruple mutant confers 150-fold higher affinity than wild-type δ, or 21-fold higher than expected for an additive increase. This further supports the hypothesis that an Asp substitution at position 178 of δ (and at the homologous positions of ϵ and γ) is required for orienting Wtx-1 in the binding site to achieve high affinity.

Residue substitution between ϵ and δ subunits suggests ion pairing between two charged residues on the receptor and a cationic moiety on Wtx-1. Replacing negatively charged ϵAsp-173 with the neutral, hydrophobic Phe or Ile likely eliminates an electrostatic attraction with waglerin, while unmasking electrostatic repulsion between ϵLys-34 and one of the seven cationic residues of Wtx-1. This may explain why the ϵD173F and ϵD173I point mutants both reduce affinity more than the ϵK34S/D173I double mutant, which simultaneously neutralizes the positive charge at ϵLys-34 and the negative charge at ϵAsp-173.

For mutations in the δ subunit, δS36K alone slightly decreases affinity, but it increases affinity only when present in the double mutant δS36K/I178D, giving a ΔG_{INT} of -1.29 kcal/mol, revealing a higher-than-expected affinity (Figure 5 and Table 5). Thus, the ϵK34S/D173I and converse δS36K/I178D double mutants each produce higher-than-additive affinities. A similar, but converse, observation is made for the $\alpha-\delta$ site selective ligand, α-conotoxin MI. The δI178F mutant (δ to γ) slightly increases affinity for α-conotoxin MI, and the δS36K mutant decreases affinity; however, the two together decrease affinity much more than predicted from the sum of the two point mutants (*13*). Thus, the mutations at δSer-36 and δIle-178 synergize to *decrease* affinity for α-conotoxin MI, but *increase* affinity for Wtx-1. These observations made with two structurally distinct ligands provide strong evidence that residues at the equivalent positions ϵ34/δ36 and ϵ173/ δ178 are close to each other in the overall structure of the respective subunits (Figure 6).

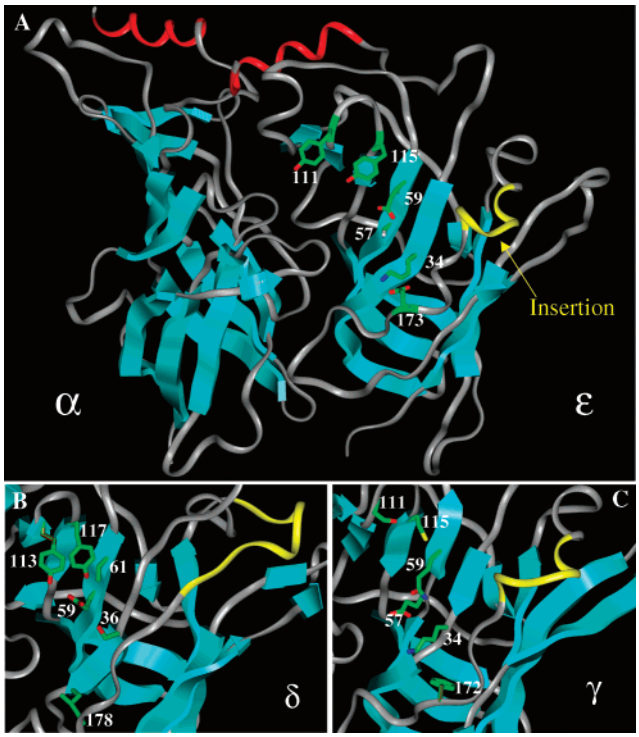

FIGURE 6: Homology model of the nAChR based on the AChBP crystal structure. (A) Model of the $\alpha-\epsilon$ interface of the receptor, with side chain positions of selectivity-determining residues shown. (B) Model of the $\alpha-\delta$ interface. (C) Model of the $\alpha-\gamma$ interface. Turquoise shows β sheet regions, red an α helix region, and yellow a region of 7−12-residue insertion in ϵ, γ, and δ subunits compared to AChBP. The coloring of the α-carbon backbone corresponds with the sequence alignment in Figure 1.

Interaction between Residues at Positions ϵ57 and ϵ173. Small, but consistent, interaction energies are found between mutations at positions ϵ57 and ϵ173 for substitutions from either δ or γ subunits. However, the interaction energy for substitutions of equivalent residues in ϵ to δ subunits is significantly greater than for substitution of equivalent residues in ϵ to γ subunits (-2.29 vs -0.54 kcal/mol). Thus,

the smaller side chains in the ϵG57D/D173I ϵ to δ double mutant may introduce less steric hindrance to bound waglerin than the ϵG57E/D173F ϵ to γ mutants. The interaction energies suggest proximity of residues at these positions, and that waglerin binding is optimized for a particular number of negative charges in the region. Other smaller interactions may exist between residues at positions 57 and 59 in the ϵ subunit (Table 4).

Distinctions in the γ and δ Templates. The interaction energies between residues further support the notion that ϵAsp-173 is critical for proper positioning of the other residues within the ϵ subunit that mediate binding site selectivity. Although some selectivity determinants differ among the ϵ, γ, and δ subunits, energetic linkages between residues at positions equivalent to ϵ-173 and residue(s) amino-terminal to it are similar in magnitude and direction regardless of whether the mutants are made in δ or ϵ subunits (Tables 4 and 5). This independence of the mutated subunit strongly suggests that the residue at position 173 governs the proper positioning of secondary residues in ϵ N-terminal to it. Although these residues differ at the $\alpha-\gamma$ and $\alpha-\delta$ binding sites, residues at the 57 and 59 positions contribute to selectivity in both γ and δ subunits, the residue at position 36 contributes in the δ subunit, and the residue at position 115 contributes in the γ subunit.

Modeling the Muscle nAChR Based on the Crystal Structure of AChBP. The recently determined crystal structure of an acetylcholine binding protein isolated from *L. stagnalis* has provided a useful template for modeling the extracellular ligand binding domain of the nAChR. The AChBP contains five identical subunits of 210 amino acids arranged in a twisted β barrel. The AChBP is most homologous to the homomeric α7 subunits of the nAChR and contains most of the hallmark residues conserved within the extracellular domain of this family of ligand-gated ion channels (Figure 1) (*4*).

We present here a homology model of the mouse muscle nAChR based on the crystal structure of AChBP. The nAChR is well modeled in most regions by homology to AChBP, since only single- or double-residue insertions are found in regions that lack α helical or β structure. However, the region between residues 159 and 175 of the ϵ subunit is not well modeled by the AChBP due to an eight-residue insertion (seven residues in γ and 12 residues in δ) compared to the AChBP (Figure 1). This insertion is particularly important for understanding binding site selectivity within the nAChR since it lodges between strands β8 and β9, and could adopt its own secondary structure. Data presented here and elsewhere (*13*, *40*, *41*) suggest that the ϵ-173/γ-172/δ-178 and ϵ-175/γ-174/δ-180 residues flanking the insertion help shape the binding site. Furthermore, residues γAsp-174/δAsp-180 have been shown to approach within 0.9 nm of the α-192/193 positions in cross-linking studies (*40*, *41*). If the $\beta8-\beta9$ insertion is modeled on the basis of the sequence alignment of the γ and δ subunits provided in ref *4*, then these residue positions would be too far away from the other binding site segments to be bridged by waglerin-1, α-conotoxin MI, and the other ligands studied previously. The accumulated experimental data suggest an altered alignment of the AChBP with the ϵ, γ, and δ subunits (Figure 1) that allows for placement of these critical residues closer to the other conserved segments contributing to the binding site (Figure 6). Thus, our model places residues 34 and 173 of the ϵ subunit close to one another, as suggested by the proximity of residues at aligned positions of the AChBP crystal structure and corroborated by the data presented here. These data enable us to place constraints on the nAChR binding site in regions of the receptor not present in AChBP.

Work in progress utilizes mutant cycle analysis to assess coupling of waglerin peptide residues with positions of the nAChR, and should delineate contact points between the receptor and this unique family of toxins.

REFERENCES

1. Corringer, P. J., Le Novère, N., and Changeux, J. P. (2000) *Annu. Rev. Pharmacol. Toxicol. 40*, 431−458.
2. Arias, H. R. (2000) *Neurochem. Int. 36*, 595−645.
3. Reynolds, J. A., and Karlin, A. (1978) *Biochemistry 17*, 2035−2038.
4. Brejc, K., van Dijk, W. J., Klaassen, R. V., Schuurmans, M., van Der Oost, J., Smit, A. B., and Sixma, T. K. (2001) *Nature 411*, 269−276.
5. Smit, A. B., Syed, N. I., Schaap, D., van Minnen, J., Klumperman, J., Kits, K. S., Lodder, H., van der Schors, R. C., van Elk, R., Sorgedrager, B., Brejc, K., Sixma, T. K., and Geraerts, W. P. (2001) *Nature 411*, 261−268.
6. Grutter, T., and Changeux, J. P. (2001) *Trends Biochem. Sci. 26*, 459−463.
7. Weinstein, S. A., Schmidt, J. J., Bernheimer, A. W., and Smith, L. A. (1991) *Toxicon 29*, 227−236.
8. Chuang, L. C., Yu, H. M., Chen, C., Huang, T. H., Wu, S. H., and Wang, K. T. (1996) *Biochim. Biophys. Acta 1292*, 145−155.
9. Sellin, L. C., Mattila, K., Annila, A., Schmidt, J. J., McArdle, J. J., Hyvönen, M., Rantala, T. T., and Kivistö, T. (1996) *Biophys. J. 70*, 3−13.
10. Molles, B. E., Rezai, P., Kline, E. F., McArdle, J. J., Sine, S. M., and Taylor, P. (2002) *J. Biol. Chem. 277*, 5433−5440.
11. Sine, S. M. (1993) *Proc. Natl. Acad. Sci. U.S.A. 90*, 9436−9440.
12. Kreienkamp, H. J., Sine, S. M., Maeda, R. K., and Taylor, P. (1994) *J. Biol. Chem. 269*, 8108−8114.
13. Sine, S. M., Kreienkamp, H. J., Bren, N., Maeda, R., and Taylor, P. (1995) *Neuron 15*, 205−211.
14. Osaka, H., Malany, S., Kanter, J. R., Sine, S. M., and Taylor, P. (1999) *J. Biol. Chem. 274*, 9581−9586.
15. Bren, N., and Sine, S. M. (1997) *J. Biol. Chem. 272*, 30793−30798.
16. Neubig, R. R., and Cohen, J. B. (1979) *Biochemistry 18*, 5464−5475.
17. Hsiao, Y. M., Chuang, C. C., Chuang, L. C., Yu, H. M., Wang, K. T., Chiou, S. H., and Wu, S. H. (1996) *Biochem. Biophys. Res. Commun. 227*, 59−63.
18. Isenberg, K. E., Mudd, J., Shah, V., and Merlie, J. P. (1986) *Nucleic Acids Res. 14*, 5111.
19. Buonanno, A., Mudd, J., and Merlie, J. P. (1989) *J. Biol. Chem. 264*, 7611−7616.
20. Yu, L., LaPolla, R. J., and Davidson, N. (1986) *Nucleic Acids Res. 14*, 3539−3555.
21. LaPolla, R. J., Mayne, K. M., and Davidson, N. (1984) *Proc. Natl. Acad. Sci. U.S.A. 81*, 7970−7974.
22. Gardner, P. D. (1990) *Nucleic Acids Res. 18*, 6714.
23. Lee, B. S., Gunn, R. B., and Kopito, R. R. (1991) *J. Biol. Chem. 266*, 11448−11454.
24. Sine, S., and Taylor, P. (1979) *J. Biol. Chem. 254*, 3315−3325.
25. Prince, R. J., and Sine, S. M. (1996) *J. Biol. Chem. 271*, 25770−25777.
26. Taylor, P., Osaka, H., Molles, B. E., Sugiyama, N., Marchot, P., Ackermann, E. J., Malany, S., McArdle, J. J., Sine, S. M., and Tsigelny, I. (1998) *J. Physiol. (Paris) 92*, 79−83.
27. Taylor, P., Molles, B., Malany, S., and Osaka, H. (2002) in *Perspectives in Molecular Toxinology* (Menez, A., Ed.) pp 271−280, John Wiley and Sons.
28. Lin, W. W., Smith, L. A., and Lee, C. Y. (1995) *Toxicon 33*, 111−114.
29. Tan, N. H., and Tan, C. S. (1989) *Toxicon 27*, 349−357.
30. McArdle, J. J., Lentz, T. L., Witzemann, V., Schwarz, H., Weinstein, S. A., and Schmidt, J. J. (1999) *J. Pharmacol. Exp. Ther. 289*, 543−550.

31. Brenner, H. R., and Sakmann, B. (1978) *Nature 271*, 366−368.
32. Schuetze, S. M., and Role, L. W. (1987) *Annu. Rev. Neurosci. 10*, 403−457.
33. Carter, P. J., Winter, G., Wilkinson, A. J., and Fersht, A. R. (1984) *Cell 38*, 835−840.
34. Quiram, P. A., and Sine, S. M. (1998) *J. Biol. Chem. 273*, 11001−11006.
35. Malany, S., Osaka, H., Sine, S. M., and Taylor, P. (2000) *Biochemistry 39*, 15388−15398.
36. Ackermann, E. J., Ang, E. T., Kanter, J. R., Tsigelny, I., and Taylor, P. (1998) *J. Biol. Chem. 273*, 10958−10964.
37. Osaka, H., Malany, S., Molles, B. E., Sine, S. M., and Taylor, P. (2000) *J. Biol. Chem. 275*, 5478−5484.
38. Hidalgo, P., and MacKinnon, R. (1995) *Science 268*, 307−310.
39. Schreiber, G., and Fersht, A. R. (1995) *J. Mol. Biol. 248*, 478−486.
40. Czajkowski, C., and Karlin, A. (1995) *J. Biol. Chem. 270*, 3160−3164.
41. Martin, M. D., and Karlin, A. (1997) *Biochemistry 36*, 10742−10750.

BI025732D